A DISTINCT PEDOGENETIC PATH UNDER A MEDITERRANEAN CLIMATE

The case of soils on Areny sandstone formation (Tremp basin, NE Iberian Peninsula)

R.M. Poch[1]
J.C. Balasch[1]
M. Antúnez[1]
J. Vadell[2]
A. Forss[2]
J. Boixadera[1,3]

[1] Departament de Medi Ambient i Ciències del Sòl, Universitat de Lleida, Catalonia, Spain

[2] Departament de Biologia, Universitat de les Illes Balears, Palma, Spain

[3] Departament d'Agricultura, Ramaderia, Pesca i Alimentació, Generalitat de Catalunya, Spain

Corresponding author
R.M. Poch, rosa.poch@macs.udl.cat

ABSTRACT
The Areny Formation is an Upper Cretaceous sandstone outcropping in the South Pre-Pyrenean area. It is composed of well-sorted quartz sand and gravel, cemented by calcite. It outcrops at a wide range of altitudes (400 to 1700 m). Soils developed on this formation in the Tremp basin (NE Iberian Peninsula) have xeric/ustic and mesic soil climate regimes. They display several soil characteristics corresponding to advanced stages of pedogenesis such as decarbonation, clay formation, and illuviation and rubefaction, ranging from Cambisols and Luvisols to Lixisols. These pedofeatures are absent in adjacent soil units of similar age, developed on finer materials, such as marls and calcareous conglomerates, where the dominant soil formation processes are carbonate translocation and weak cementation. These neighbouring soils are mainly Calcisols, some of them with a petrocalcic horizon. Six profiles formed on the Areny sandstone were selected for an in-depth study of their soil formation processes. A multi-scale approach, from geomorphological to micromorphological analyses, was employed. The soils have a neutral to slightly acidic reaction in the Bt horizons, with loamy sand textures and a clay content of 10 % that appears completely as illuviated clay in the thin section; reddish hues (2.5YR) and high chromas, the absence of calcite in the upper horizons or in the whole profile, and the presence of iron pans in some locations. Amorphous iron is found in low amounts compared to Fe in silicates and as finely crystalline forms. The latter increases with depth in the decarbonated profiles. The high weathering degree of the oldest profiles is shown by kaolinite being the dominant clay, which was probably inherited from the pre-Quaternary period. The clay fraction also contains remarkable amounts of mixed layers chlorite/smectite, chlorite/vermiculite or illite/smectite, which may be considered products of present-day pedogenesis. The geomorphological analyses allowed us to determine the ages of the surface formations of four of the profiles (50 to more than 350 ky), which indicated much faster soil formation rates than those reported in similar Mediterranean environments. Thus, the proposed stages of soil evolution in these sediments imply a fast decarbonation, followed by clay formation, and illuviation. These processes have strong implications in establishing the soil-landscape relationships in the area.

KEYWORDS
carbonate, decalcification, rubefaction, clay illuviation, clay formation, Catalonia

DOI
10.5281/zenodo.3420951

ORCID
R.M. Poch: 0000-0001-8639-4204
J.C. Balasch: 0000-0001-5970-1918
M. Antúnez: 0000-0001-8509-9086
J. Vadell: 0000-0002-0980-4908
J. Boixadera: 0000-0002-0258-0761

1. Introduction

Soils under Mediterranean environments do not undergo specific soil formation processes different from other climates, although it is recognized that they do have a particular set of common soil formation factors in several parts of the world such as the Mediterranean climate (warm and dry summer), the presence of carbonate rocks, steep slopes and – in the Mediterranean – the supply of Saharan dust and a long-lasting anthropic influence (Yaalon, 1997). The resulting processes are moderate weathering, 2:1 clay illuviation, hematite-induced reddening, and carbonate redistribution (Yaalon, 1997; Bech et al., 1997; Fedoroff and Courty, 2013). Even so, the present or palaeo-character of these processes is not completely understood. According to Fedoroff (1997), clay illuviation is only active in the northern, wetter margins of the Mediterranean basin and should be considered a palaeofeature in the rest of the region. Indeed, the alternation of wetter/drier climates during the Quaternary has been claimed as a driver of decarbonation, clay illuviation, and reddening/recarbonation in several Mediterranean chronosequences (e.g. Sauer et al., 2010; Poch et al., 2013; Fedoroff, 1997; Darwish and Zurayk, 1997).

One of the tasks of pedogenetic analysis is the establishment of the relationship between soil age and formation degrees, which is normally defined regionally, taking into account climatic variables (Sauer et al., 2006). These relationships do not always apply because of external inputs (such as dust) or outputs (mainly erosion) (Scarciglia et al., 2015); additionally, soil evolution is not uniform, but subjected to internal thresholds and feedback mechanisms (Sauer et al., 2006), as it occurs with clay illuviation and rubefaction taking place after decalcification.

The Tremp basin is located in the Pre-Pyrenean area, north-east of the Iberian Peninsula, on a sliding mantle formed by calcareous Cretaceous and Tertiary materials, resulting from the uplift of the Pyrenees. The climate is Mediterranean semi-arid. The surface formations of known age are the Segre river terraces and several levels of travertine mounds equivalent to those of large alluvial fans covering the basin, which were formed during the Middle and Upper Pleistocene. Detailed soil surveys of this area revealed the presence of strongly expressed contrasting processes (calcium carbonate accumulation/cementation and clay illuviation/reddening) on adjacent surfaces of similar ages (Porta et al., 2013), but that were developed on different parent materials. In particular, soils formed on Areny sandstones (Upper Cretaceous sandstone, made of quartz sand cemented by calcium carbonate) are redder and more acidic than surrounding soils and may show clay illuviation, while petrocalcic horizons are found on adjacent pediment surfaces at the same level. Bech et al. (1985) noted different degrees of decarbonation, reddening, and clay illuviation on neighbouring soils in the area and attributed this to the different parent materials of the soils.

The objective of this research is to determine the role of the parent material (Areny sandstone) on soil formation processes (clay illuviation and reddening) in order to establish the present or palaeo character of these soil-forming processes, following a multi-scale approach; and to discuss the correlation of the degree of expression of these processes with age and with neighbouring soils on geomorphic positions of a similar age undergoing very different pedogenetic processes.

2. Material and methods

2.1. PHYSICAL ENVIRONMENT

The Pyrenees are a mountain range of the Alpine folding, which is over 1500 km in length. It is the result of the continental drift of the Iberian Plate during the Mesozoic and its final collision with the European Plate during the Cenozoic. This uplift caused the formation of several landslide mantles that make up the Pre-Pyrenees, South of the Axial Zone, formed by rocks of the Mesozoic and Paleogene, which determine several mountain ranges of east-west orientation. The Tremp Basin (Conca de Tremp) is one of the intra-mountain basins between them, south of the main axis of the Pyrenees, where it is possible to find sediments and structures of previous palaeoenvironments. Its width is approximately 50 km, with altitudes ranging between 400 m in the centre and nearly 1700 m at the margins.

The climate is mountainous Mediterranean, with an annual precipitation between 580 and 750 mm that follows an altitudinal gradient and a bimodal distribution along the year (spring and autumn), with a severe summer drought. The mean annual temperatures are between 12.8 °C at the valley bottom and 8.4 °C at the highest altitudes, which have common snow events every winter. Soil moisture and temperature regimes in the region are Xeric/Ustic (below and above ca. 1000 m) and Mesic respectively (SSS, 2014).

The soils are mainly formed on highly calcareous materials of different nature, from sandstones to clays and travertines. Calcium carbonate redistribution is very common, from calcic to petrocalcic horizons developed on old alluvial fans (Machette stages II to IV; Machette, 1985; Porta et al., 2013). At the valley bottom, soils with gypsum accumulations and vertic features are present, probably inherited from the colluvium of the Garumnian (Upper Maastrichtian) marls (Porta et al., 2011). The presence of travertines is also noteworthy since they are very important in the centre of the basin, due to springs originating from the underlying confined aquifer (Linares et al., 2010).

It is composed from a series of relict tufa mounds older than 350 ky BP and a lower tufa unit associated with current groundwater aquifer outlets (Basturs Lakes), which have been active since 106 ky BP during both cold and mild Marine Isotopic Stages (MIS) (Pellicer et al., 2014).

The main land use in the basin is forestry. Agriculture is concentrated on valley bottoms around the main villages and on the plains close to rivers. Besides cereals and alfalfa, both rainfed and irrigated, traditional almond and olive trees can also be found. There has been a recent increase of vineyards, included within the Costers del Segre Appellation d'Origine wines. The occupation of the land dates back to at least the end of the Middle Pleistocene, as illustrated by the Nerets Archaeological site on the soils of the Areny sandstones, where lithic artefacts can be found along the whole slope due to the erosion of the original red soils (Rodríguez and Rosell, 1993). The first large-scale transformation of the landscape was due to the Roman rule that brought a new territorial organization and a complex administrative framework (Iber – Roman period, 650 BC - 450 AD). This occurred along the old optimum climate and permitted the expansion of crops throughout the territory.

2.2. THE ARENY FORMATION

The Areny sandstones in the Conca de Tremp mark the transition from marine (marls of the Upper Maastrichtian, locally named Garumnian) to continental environments (Cretaceous–Tertiary) (Oms et al., 2016). As such, they are calcarenites, formed by deltaic quartz sand derived from the weathering of the igneous rocks of the axial Pyrenees and cemented by carbonates. The average thickness of the Areny formation is about 500 m and it outcrops at the margins of the basin (Figure 1).

Regarding its composition, the quartz content in the calcarenite samples decreases regularly from 40.5 % at the bottom to 17.5 % at the top (Nagtegaal, 1972). The quartz grains are rounded and well-sorted. Among the carbonate grains, well-rounded calcareous algal fragments (rhodophyceans) and larger Foraminifera (Orbitoides, Siderolites) are particularly abundant. Other grains include pelecypod and echinoderm fragments, *Radiolitella pulchellus* (Vidal) rudists (hippuritids), pelecypod debris, and corals (Mey et al., 1968; Nagtegaal, 1972; Villalba-Breva et al., 2015). This formation underwent an early complex diagenetic process, consisting of a first stage of marine and meteoric cementation (development of ferruginous rims and

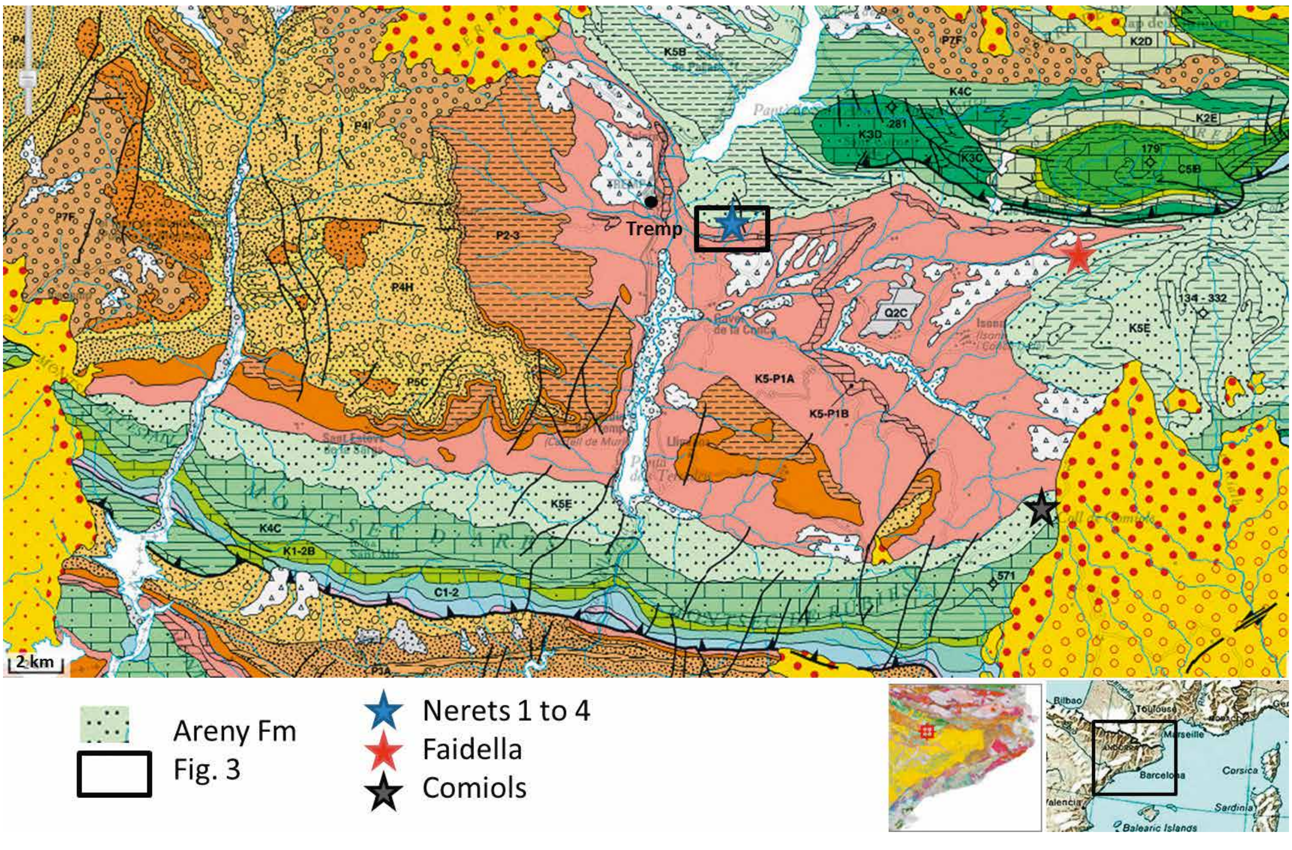

Figure 1. Geological map of the Tremp basin and profile location. Source and complete legend: ICGC http://www.icc.cat/vissir3/llegendes/mgc250m.pdf.

Table 1 Main site characteristics of the studied profiles

Profile	Altitude (m asl)	Slope and aspect	Landform	Parent material	Vegetation
Faidella	1170	15 %, NW	Middle slope	Calcareous (Areny Formation) sandstone	Afforestation. *Pinus sylvestris, Quercus ilex sp. Ballota; Erica scoparia, Juniperus communis, Genista scorpius, Artostaphylos uva-ursi, Genista hispanica, Lavandula angustifolia, Globularia vulgaris, Calluna vulgaris.*
Comiols	1099	10 %, W	Upper slope		
Nerets 1	584	10% N	Upper alluvial fan	Pedosediment from the Areny sandstone	*Quercus ilex, Thymus vulgaris, Rosmarinus officinalis.*
Nerets 2	577	15% N	Upper alluvial fan		
Nerets 3	545	3% S	Lower alluvial fan		*Quercus rotundifolia, Rosmarinus officinalis.*
Nerets 4	515	2% S	Lower alluvial fan		*Quercus faginea, Genista scorpius, Rubia peregrina.*

precipitation of druse calcite), followed by pedogenesis. The latter is shown through the corrosion and dissolution of carbonate grains and of previous cements, which led to the fragmentation, brecciation, nodulisation, and ferruginisation of the former lithified beach sand, creating a secondary porosity of vughs and fractures (Díaz-Molina et al., 2007).

The Nerets range, about 2.5 km East of Tremp, constitutes the western edge of the northern flank of the Tremp Syncline. It is formed by a sub-structural slope, excavated in the quartz sandstones of the Areny Formation, dipping ca. 15º S. At its footslope, just in contact with the loose materials covering the sandstones (basal part of the Tremp Formation, Maastrichtian, Rosell et al., 2001), there are two sets of alluvial fans attached to the slope, stepping at different altitudes.

2.3. METHODS

The geomorphological analysis of the alluvial fans of the Nerets site was based on geomorphological mapping techniques, granulometric and sediment analysis of alluvial bodies, and on dating in comparison with local deposits of similar characteristics with absolute dating. The geomorphological mapping of the quaternary alluvial bodies allowed us to determine the shape and surface extent of the formations and the spatial and temporal relationships between them and any older neighbouring substrates. The sedimentary analysis of the variations of particle size in the interior of the alluvial fans allowed us to determine the proximity or distance of the materials with respect to the source areas. Dating was determined through stratigraphic correlations, which allowed us to determine the approximate age of formation of the Nerets alluvial fans relative to similar sediments, dated through radio-isotope techniques of uranium and radiocarbon.

Six soil profiles, located at different sites within the Areny formation-outcrops or derived alluvial fans (Figure 1), were described and sampled for chemical, mineralogical, and micromorphological analyses. Two of them (Faidella and Comiols) are located at higher altitudes on the in situ weathering products of the sandstone. The other four were located (Nerets 1 to 4) on a system of alluvial fans (Nerets site) made of pedosediments from the sandstone outcrops north of the basin (Nerets range). Their main characteristics are found in Table 1.

Additionally, rock fragments were sampled for mineralogical, micromorphological, and chemical analyses. The profiles were described following the guidelines of SINEDARES (CBDSA, 1983). Undisturbed samples were collected at selected profiles and horizons for micromorphological analyses. The physicochemical analyses of the profiles was done according to MAPA (1993). Particle size distribution was determined by the pipette method, after the removal of organic matter with H_2O_2 and dispersion with Na-hexametaphosphate. Cation exchange capacity was determined by displacement with 1 M NH_4OAc (pH 7) and the exchangeable cations were measured by atomic absorption. Organic carbon was determined following the Walkley-Black method. Soils were classified according to Soil Taxonomy (SSS 2014) and WRB (IUSS Working Group WRB, 2015).

Total iron (Fe_t) was determined after digestion with HCl and HNO_3. Dithionite soluble Fe (Fe_d) was determined with dithionite citrate, buffered with the sodium bicarbonate method according to Mehra and Jackson (1960). Oxalate extractable Fe (Fe_{ox}) and Al (Al_{ox}) were determined through extraction with acid ammonium oxalate 0.2 M at pH 3 (Schwertmann, 1964). In all extracts, Fe was determined by atomic absorption.

Reddening was assessed as a colour (moist) index; the redness index has the following equation:

$$RI= [(10\text{-}nhue) * chroma]/value$$

from Torrent (1983) with the constant nhue value being: 10YR = 10; 7.5YR = 7.5; 5YR = 5; 2.5YR = 2.5; 10R = 0.

We calculated the Fe-index (Wagner et al., 2014), defined by the following equation:

$$\text{Fe index} = (\%Fe_d - \%Fe_{ox})/(\%Fe_t/\%Clay)$$

Micromorphological analyses were performed in some of the profiles according to the procedures of Benyarku and Stoops (2005) for making vertical thin sections, 13 cm long and 5.5 cm wide, from air-dried, undisturbed soil blocks. Stoops' (2003) guidelines were followed for their description and study.

Semi-quantitative clay mineralogy of the selected samples (powder and oriented air-dry aggregates) was carried out through X-ray diffraction, using a Siemens D-5000 diffractometer. The mineralogy of the skeleton grains of the Areny sandstone (volume %), sampled at the Faidella site, was done through point-counting of 250 grains. The elementary composition of the same set of samples was determined by digestion in *aqua regia* mixture and determined by ICP-OES (Optima 5300DV, PekinElmer).

The Chemical Index of Alteration (CIA, Nesbitt and Young, 1982) and Chemical Index of Weathering (CIW, Harnois, 1988) were calculated as $CIA = Al \cdot 100/(Al+Ca+K+Na)$ and $CIW = Al \cdot 100/(Al+Ca+Na)$. The Weathering index (WI, Price et al., 1991) was calculated for Comiols and Faidella in reference to their respective underlying sandstones as $WI = R_{sample}/R_{reference}$, where $R = Al/(Ca+Na)$.

3. Results

3.1. MINERALOGY AND PETROGRAPHY OF THE ARENY SANDSTONE

The composition of the Areny calcarenite is mainly calcium carbonate, either as cement (micrite and microsparite) or as calcite grains and fossils. The mineralogical analyses of one sample shows that the non-calcareous mineral grains are 39.2 % (weight), after removal of calcite (calcareous cement and calcareous sand). They are comprised of rounded quartz and quartzite grains (92.8 % vol) with minor amounts of other minerals (Figure 2a). Among them, the few plagioclases (1.6 % vol) and microclines (1.2 % vol) show a first stage parallel linear and crossed linear alteration to calcite (Figs. 2 b, c, d), according to the weathering path described for igneous rocks in Iran (Yousefifard et al., 2015). There are few chlorites (3.6 % vol) and biotites (0.8 % vol), as noted by Bech et al. (1985).

3.2. GEOMORPHOLOGY OF THE NERETS SITE

The profiles at the Nerets site are located on two alluvial fans (Figure 3). The upper fan level has a very small extension with a single outcrop of about 500 m long, parallel to the slope and 100-200 m wide. It is located just above and west of the Les Arenes quarry at an altitude of between 560 and 580 m. It consists of a very regular reddish level, about 8-10 m thick, with iron-rich quartz sand, accompanied by some well-rounded sandstone gravels, a few cm in diameter. Its surface dips 10 % to the south.

In the distal part, this fan level is penetrated and passes laterally to a level of calcareous gravels and boulders with some blocks with a certain degree of bedding that corresponds to the continuation of the oldest alluvial cones described in the Tremp basin (defined as Qv5; ICGC, 2007), whose closest remains would be at the top of the hill of the Sant Miquel hermitage, NE of Suterranya (Figure 3).

This upper level originated through the denudation and accumulation of sands and clays from the alteration

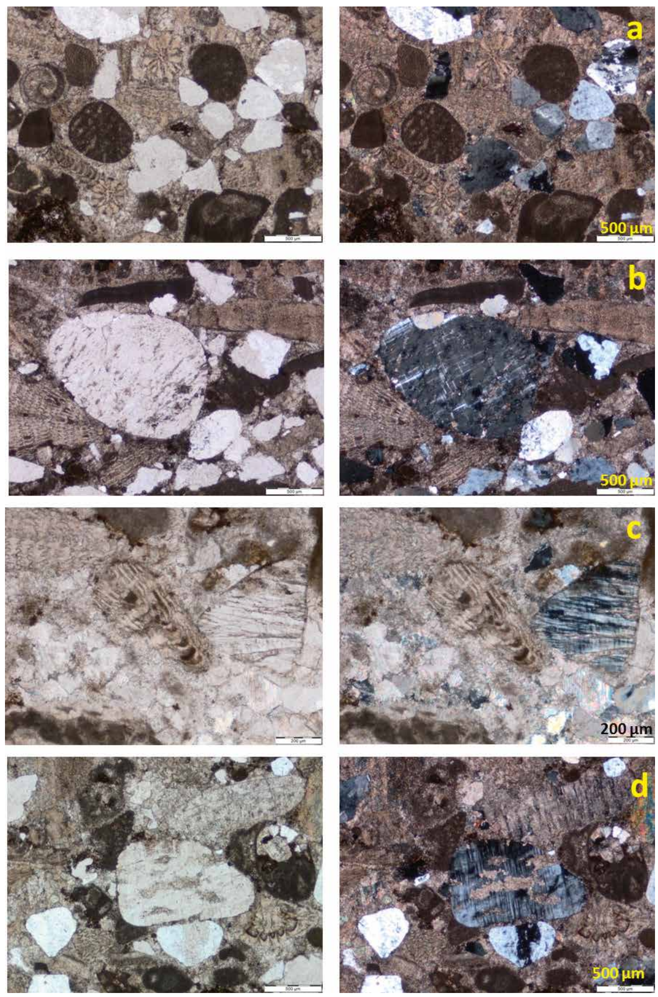

Figure 2. Micromorphology of the Areny calcarenite.

a. general appearance: note the abundance of fossils
b. and c. round microcline sand grains with slight cross linear and parallel linear weathering patterns
d. dotted alteration to micrite in a plagioclase

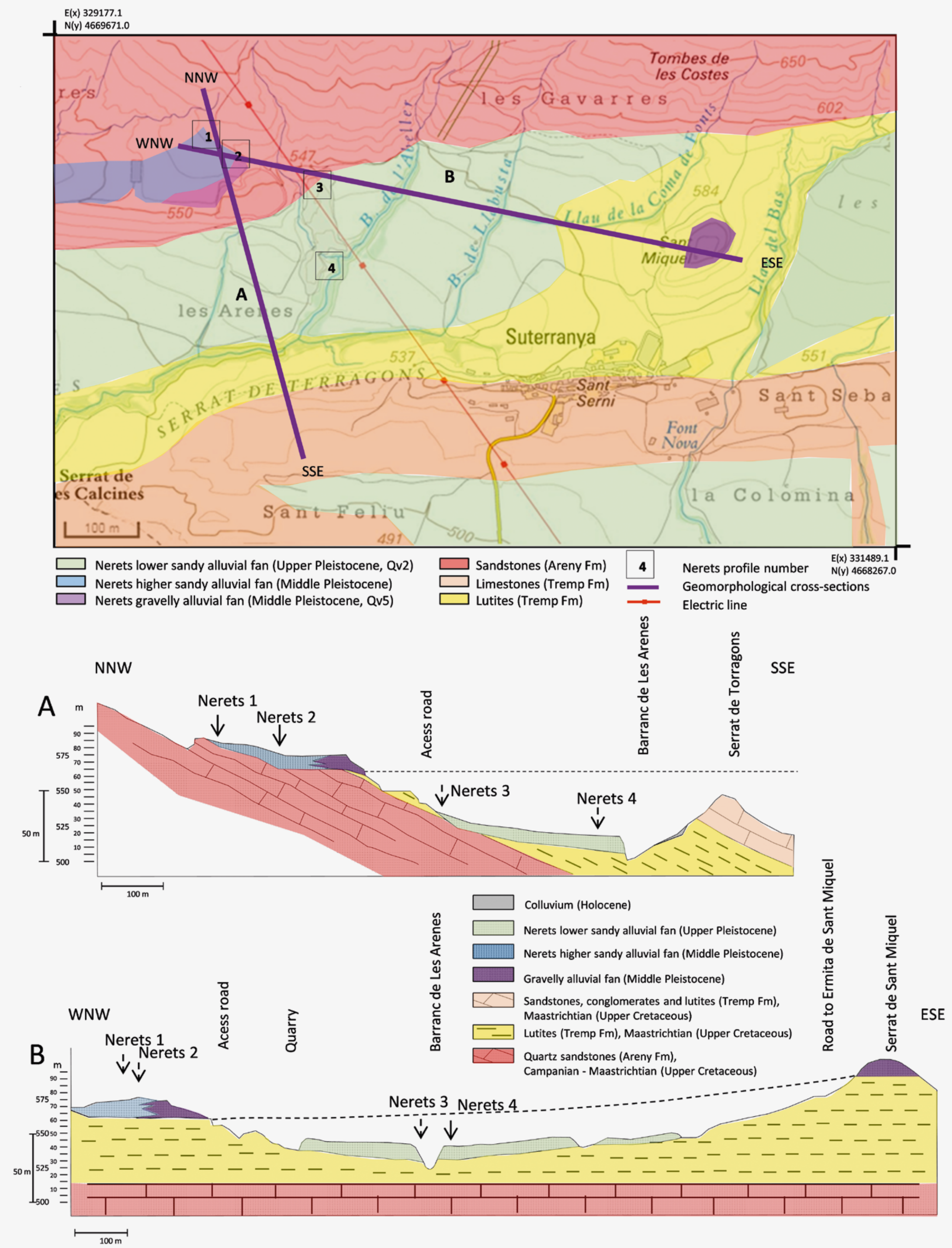

Figure 3. Geomorphological map and sections of the Nerets site (modified from ICGC, 2007).

and decomposition of the remains of the Areny sandstone at the footslope of the Nerets range. The karstification of the sub-structural surface of the Nerets range favoured the formation of rubefacted soils and the loosening of the sand grains forming the sandstones. The decomposition process was of a very high intensity, since there are no remains left other than the quartz granular components.

Its approximate age can be calculated through its correlation with the well-dated sets (U/Th series) of carbonate tobas (travertines) of the Basturs lake system covering them. The dating of Tufa 1 (the oldest one) that covers the Qv5 level is more than 350 ky (Pellicer et al., 2014), therefore the Qv5 level would be older. Materials on higher levels are synchronous to the deposition of the Qv5 level and, consequently, are considered the same age (> 350 ky) and thus attributed to the Middle Pleistocene.

The lower alluvial fan level covers the entire bottom (Figure 3) of the broad valley between the Nerets range and the reliefs of Suterranya at a height that oscillates between 550 and 500 m. At the southern side of the reliefs of Suterranya, this level can be correlated with the set of alluvial fans with a different composition that is defined as Qv2 (ICGC, 2007). The lower level shows very interesting outcrops in the Les Arenes quarry that produces loose quartz sands. The surface dips 11 % to the south.

The sediments of this fan are formed, as in the upper one, by quartz sands with scattered gravels of well-rounded quartz and red fine material. The lower fan has a maximum thickness of 2-3 m in the proximal part (apex) and 10-12 m in the central and distal parts.

This lower fan presents a clear correlation with the Qv2 surface formation materials (ICGC, 2004 and 2007), that are correlated with the T2 terrace of the Noguera Pallaresa River. In Basturs, the travertines of Tufa 3 (the lowest) are dated around 100 ky (Pellicer et al., 2014) and cover the Qv3 cone, at a higher level than the Qv2. Therefore, the age of Qv2 materials is much younger. On the other hand, the T2 terrace, located about 20-24 m above the Noguera Pallaresa river bed, has an Upper Pleistocene age (ICGC, 2004). In the Segre-Cinca system, this terrace has an age of about 50 ky (dated with OSL, Sancho et al., 2007; Lewis et al., 2009). In conclusion, we calculate the age of this lower fan to be around 50 ky.

The surfaces of the two alluvial fans have a height difference of about 40 m, which represents the erosion that separates them in the evolution of the drainage network. The sand level of the upper fan adjusts to the base level of the drainage network, excavated in the Dellà Basin in the Middle Pleistocene. As can be seen in the A section (Figure 3), this base level goes through the reliefs of Suterranya and connects with the slope of the wide valley of the Abella and Conques rivers. At that moment, the valley of Barranc de l'Abeller did not exist.

3.3. SOIL MORPHOLOGY AND PHYSICOCHEMICAL CHARACTERISTICS

The morphology of the profiles (Table 2) shows the development of B horizons and rubefaction (hues 2.5 and 5YR) in Comiols (Bw) and Nerets profiles (Bt, Btk, Bk, Bwk), while the Faidella profile only has very sandy Bw horizons and contains a buried profile without rubefaction. Redoximorphic features, as small mottles, are only observed at the bottom of Nerets 1.

All the Bt horizons described in the field correspond to an increase in the clay fractions (Table 3). These increases allow them to qualify for argillic horizons (SSS, 2014). Otherwise, the textures are sandy to sandy loam. Although Comiols, Faidella, and Nerets 1 are completely decarbonated (Table 2), only the Faidella profile has an acidic reaction throughout and the lowest base saturation (V=52 % at the surface, Table 3), followed by Nerets 1, which is partly desaturated (V between 80-90 %). Nerets 2 is decarbonated and Nerets 3 and 4 are partly decarbonated at the top horizons, but not decalcified since all of them have base saturations of nearly 100 %. In the case of Nerets 2, the underlying horizons show recarbonation processes, probably inherited from the dynamics in the fan. A clear colluvic character is observed in Faidella profile. Nerets 3 and 4 present frequent queras: biocalcifications similar to pseudomycelia, but composed of calcite pseudomorphs after root cells (Herrero et al., 1992). Besides the downward leaching of carbonates within the profiles, their accumulation within the fans proceeds roughly to the lowest (distal) sections, creating a complex spatial pattern with high variability in short distances. In spite of that, the lower boundary of the decarbonated horizons is clearly deeper in the upper fan (more than 1m) than in the lower one (about 40 cm, Table 2), which we can relate to their age.

Table 4 displays the different content of iron oxides of the studied soils as well as their ratios. The total iron strongly differs between and within profiles. In Nerets 1, it clearly increases with depth, but it does not follow the same trend in the rest of the profiles. Crystalline Fe (Fe_d-Fe_{ox}) of Nerets 2 tends to be lower in the carbonated horizons, but this trend does not apply to Nerets 3 and 4, with Fe contents unrelated to depth or to carbonate content. Nerets 3 and 4 have very high values of Fe_d/clay in the Bt horizons, which suggests a pedosedimentary origin of the parent materials. The Nerets1 profile shows the clearest weathering sequence: the amount of Fe-oxides (Fe_d-Fe_{ox}, hematite and goethite) and proportion of pedogenic iron (Fe_{ox}/Fe_d) increases in depth. Clear lithologic discontinuities are observed in Faidella and Nerets 2, 3 and 4, expressed as anomalous sequences of those indices, but all of them within the same range of values. This observation is in accordance with the colluvial material in Faidella and the

Table 2 Selected morphological characteristics of the profiles

Profile and horizon	Depth (cm)	Munsell colour (moist)	Redness Rating*	Structure	Mottles	Reaction to HCl	Pedofeatures
Faidella							
Oi	-4- -3	-	-	-	-	-	-
Oe	-3-0	-	-	-	-	-	-
A	0-20	10YR 5/2	0.0	vw, cr, f	none	none	none
Bw	20-48	7.5YR 5/4	2.0	w, sab, m	none	none	none
Ab	48-65	7.5YR 4.5/3	1.7	vw, cr, m	none	none	none
ABb	65-82	7.5YR 5/6	3.0	w, sab, m	none	none	none
Bwb	82-110/120	7.5YR 5/8	4.0	w, sab, f	none	none	none
R	>110/120	-	-	-	-	-	-
Comiols							
O	-1-0	-	-	-	-	-	-
A	0-15	2.5YR 3/3	7.5	mod, cr, m	none	none	none
AB	15-28	2.5YR 3/4	10.0	mod, sab, c;	none	none	none
Bw	28-80	2.5YR 4/6	11.3	faunal	none	none	Very few clay coatings
C	80-150	5YR 5/8	8.0	mod, sab, c	none	none	Very few clay coatings
Nerets 1							
A	0-11	2.5YR 5/4	6.0	vw, sab, m	none	none	none
AB	11-25	2.5YR 5/8	12.0	vw, sab, m	none	none	none
Bt1	25-42	2.5YR 5/8	12.0	vw, sab, c	none	none	Frequent clay coatings
Bt2	42-75	2.5YR 4/8	15.0	vw, sab, c	none	none	Abundant clay coatings
Bt3	75-113	2.5YR 4/6	11.3	w, sab, c	very few, Mn	none	Continuous clay coatings
Bt4	113-140	2.5YR 4/8	15.0	w, sab, c	very few, Mn	none	Abundant clay coatings
Nerets 2							
Bt	0-40/150	2.5YR 5/6	6.0	w, sab, m	none	none	Abundant clay and silt coatings
2Btk1	40/150-155/160	5YR 5/8	8.0	-	none	none	Few clay and silt coatings. Carbonate pseudomycelia, hard carbonate nodules.
2Bk2	155/160-160/200	-	-	apedal	none	very strong	Carbonate pseudomycelia and rhyzocretions.
3Bk3	160/200->230	5YR 5/8	8.0	apedal	none	very strong	Carbonate pseudomycelia and rhyzocretions
Nerets 3							
Oa	-1-0	-	-	-	-	-	-
A	0-9	5YR 3/4	6,7	m, cr, f	none	weak	none
Bt	9-38/49	2.5YR 4/5	9,4	m, sab, m	none	weak	Clay coatings
2Bwk1	38/49-41/70	5YR 5/6	6	m, sab, c	none	very strong	Frequent carbonate pseudomycelia and
2Bwk2	>41/70	5YR 4/6	7.5	m, sab, c	none	very strong	queras.
Nerets 4							
A	0-8	5YR 5/6	6.0	m, cr, f	none	none	none
Bt	8-36	2.5YR 4/6	11.3	m, sab, m	none	none	Few clay coatings around quartz grains
2Bk	36-127	7.5YR 6/6	2.5	vw, sab	none	very strong	Carbonate pseudomycelia and few queras
3Bwk	127-177	7.5YR 5/6	3.0	w, sab	none	very strong	Carbonate pseudomycelia, abundant queras and very abundant rhyzocretions (cm in size)
4Bk	177->277	10YR 6/6	0.0	w, sab	none	very strong	Generalized carbonate accumulation

vw: very weak; w: weak; mod: moderate; str: strong; sab: subangular blocky; cr: crumb; c: coarse; m: medium; f: fine
* Torrent (1983)

Table 3 Main chemical properties of the profiles

Profile and horizon	pH H_2O 1:2.5	$CaCO_3$ eq. (%)	OM (%)	Clay < 2µm	Fine Silt 2-20 µm	Coarse Silt 20-50 µm	Fine Sand 50-500 µm	Coarse Sand 0.5-2 mm	Texture	CIC (cmol+/kg)	CIC clay (cmol+/kg)	V%
				(%)								
Faidella												
A	5.1	0	0.97	2.4	2	1.5	11.6	82.5	S	2.4	98.1	52
Bw	5.8	0	0.38	2.7	1.8	0.5	11.1	83.9	S	1.6	58.5	68
Ab	6.6	0	0.45	3.9	3.9	1.3	10.8	80.1	S	2.1	52.9	93
Bwb	7.0	0	0.28	8.4	2.6	0.8	11.9	76.3	LS	2.4	28.0	100
Comiols												
A	7.5	0	2.89	7.5	6.9	2.2	16.2	67.2	LS	8.8	111.6	100
AB	8.1	0	1.33	13.3	7.1	2.6	19.1	57.9	LS	6.9	49.2	100
Bw	8.0	0	0.29	20.2	3.4	1.8	11.2	63.4	CL	7.6	37.0	100
C	8.1	0	<0.14	6	5.2	1.9	19	67.9	LS	1.6	26.4	100
Nerets 1												
A	7.1	0	1.1	6.9	1.1	3.4	40.2	48.4	S	2.7	36.9	100
AB	6.0	0	0.6	8.4	1.1	3.0	33.0	54.6	S	2.3	26.2	72
Bt1	7.2	0	-	11.1	2.1	3.4	43.5	40.0	LS	2.1	18.9	100
Bt2	6.7	0	-	10.1	1.1	3.7	45.9	39.1	LS	2.5	24.8	87
Bt3	6.4	0	-	18.2	2.7	3.1	25.5	50.6	SL	6.6	36.3	85
Bt4	6.1	0	-	17.3	1.1	3.0	36.3	42.2	SL	5.2	30.1	80
Nerets 2												
Bt	8.4	0	0.4	16.2	1.1	1.9	31.7	49.1	SL	5.6	33.8	100
2Btk1	7.2	0	0.5	18.2	2.1	2.7	34.7	42.4	SL	5.5	29.2	100
2Bk2	8.7	4.4	-	7.5	1.3	1.8	16.7	72.7	S	3.8	50.7	100
3Bk3	8.5	4.7	-	4.2	2.8	2.5	38.5	51.9	S	3.9	92.9	100
Nerets 3												
A	8.4	2	0.67	12.5	7.1	7.9	8.1	64.4	SL	6.6	51.5	99
Bt	8.5	3	0.36	22.3	7.1	8.4	8.2	54	SCL	9.9	43.7	100
2Bwk1	8.5	18	0.2	10.1	12	11	12.2	54.7	SL	5.1	50.1	100
2Bwk2	8.5	10	0.05	10.2	8.1	8.1	9.8	63.8	SL	3.4	33.2	100
Nerets 4												
A	7.6	1	2.22	6.9	3.6	4.9	20	64.6	LS	5.4	73.8	100
Bt	7.6	0	0.68	17	6.1	6.4	12.9	57.6	SL	8.2	46.9	100
2Bk	8.5	8	0.01	7.9	6.3	5.3	9.2	71.3	LS	2.9	36.7	100
3Bwk	8.6	8	0.1	14	10.1	8.1	12.2	55.6	SL	6.8	48.4	100
4Bk	8.2	23	0.1	12.3	9.3	6.6	9.3	62.5	SL	4.9	39.6	100

Table 4 Extracted iron composition of the profiles

Profile and horizon	Fe_{ox} (%)	Fe_d(%)	Fe_t (%)	Fe_{ox}/Fe_t	Fe_d/Fe_t	Fe_{ox}/Fe_d	Fe_d-Fe_{ox}	Fe_t-Fe_d	(Fe_d-Fe_{ox})/Fe_t	Fe_d/clay	Fe index*
Faidella											
Bw	0.029	0.340	0.390	0.074	0.872	0.085	0.311	0.050	0.797	0.126	2.5
Bwb	0.040	0.950	1.320	0.030	0.720	0.042	0.910	0.370	0.689	0.113	8.1
Comiols											
Bw	0.029	2.150	2.420	0.012	0.888	0.013	2.121	0.270	0.876	0.106	19.9
C	0.007	1.180	1.170	0.006	1	0.006	1.173	0	1	0.197	6.0
Nerets 1											
A	0.007	0.270	0.480	0.015	0.563	0.026	0.263	0.210	0.548	0.039	6.7
AB	0.010	0.376	0.722	0.014	0.521	0.027	0.366	0.346	0.507	0.045	8.2
Bt1	0.016	0.660	0.919	0.017	0.718	0.024	0.644	0.259	0.701	0.059	10.8
Bt2	0.020	0.652	0.799	0.025	0.816	0.031	0.632	0.147	0.791	0.065	9.8
Bt3	0.050	1.366	1.738	0.029	0.786	0.037	1.316	0.372	0.757	0.075	17.5
Bt4	0.031	1.031	1.290	0.024	0.799	0.030	1.000	0.259	0.775	0.060	16.8
Nerets 2											
Bt 0-30 cm	0.036	1.009	1.499	0.024	0.673	0.036	0.973	0.490	0.649	0.062	15.6
Bt 90-120 cm	0.035	1.033	1.455	0.024	0.710	0.034	0.998	0.422	0.686	0.057	17.6
2Bk2	0.023	0.522	0.830	0.028	0.629	0.044	0.499	0.308	0.601	0.070	7.2
3Bk3	0.036	0.375	0.528	0.068	0.710	0.096	0.339	0.153	0.642	0.089	3.8
Nerets 3											
A	0,045	0,857	1,217	0.037	0.704	0.052	0.812	0.360	0.667	0.069	11.8
Bt	0,078	1,291	2,016	0.039	0.640	0.061	1.212	0.725	0.601	0.103	11.7
2Bwk1	0,029	0,775	1,222	0.024	0.634	0.037	0.746	0.447	0.611	0.035	21.5
2Bwk2	0,048	0,820	1,525	0.032	0.538	0.059	0.772	0.705	0.506	0.081	9.5
Nerets 4											
A	0,033	0,581	0,921	0.036	0.631	0.056	0.549	0.340	0.596	0.057	9.6
Bt	0,053	1,147	1,387	0.039	0.827	0.047	1.094	0.240	0.788	0.166	6.6
2Bk	0,017	0,533	0,832	0.020	0.641	0.031	0.517	0.299	0.621	0.077	6.7
3Bwk	0,043	0,869	1,820	0.023	0.477	0.049	0.826	0.951	0.454	0.051	16.2
4Bk	0,035	0,566	0,891	0.039	0.635	0.061	0.531	0.325	0.596	0.072	7.4

ox: extracted with (oxalic acid+ ammonium oxalate) 0.2M pH 3; d: extracted with Na citrate, Na bicarbonate and Na dithionite; t: total digestion with HCl and HNO_3

*Wagner et al., 2014.

Table 5 Elemental composition of the profiles (macro-elements, values in g/kg) and different weathering indices

	Ca	Mg	K	Al	CIA[1]	CIW[2]	WI[3]	Ti/V
Faidella								
Bw	0.2	0.5	2.4	5.6	68.1	96.2	219.2	11.0
Bwb	0.8	1.5	2.4	13.2	80.2	93.9	121.5	10.1
Sandstone	214.9	2.6	0.4	3.7	1.7	1.7		4.8
Comiols								
Bw	2.2	1.0	1.2	18.2	82.6	87.5	68.7	4.1
C	0.6	0.4	3.4	16.1	79.9	95.8	205.0	6.2
Sandstone	300.7	0.8	1.1	3.2	1.1	1.1		3.8
Nerets 1								
A	0.9	0.7	4.6	10.9	66.0	91.5		17.8
AB	0.3	0.5	1.5	10.7	85.3	96.5		16.9
Bt1	0.6	0.8	1.7	16.2	86.9	95.9		19.3
Bt2	0.5	0.7	4.9	15.3	73.5	96.0		16.1
Bt3	1.4	2.1	4.7	34.2	84.5	95.6		10.3
Bt4	0.8	1.4	6.6	29.9	79.8	96.9		11.1
Nerets 2								
Bt	1.9	1.4	8.7	27.0	71.4	92.6		11.7
2Btk1	1.0	1.6	7.9	27.9	75.2	95.7		13.8
2Bk2	14.0	1.3	4.9	19.4	50.4	57.8		15.2
3Bk3	17.7	0.8	1.2	14.4	43.2	44.8		23.5

[1]Chemical index of alteration (Nesbitt and Young, 1982);
[2]Chemical index of weathering (Harnois, 1988);
[3]Weathering Index (Price et al., 1991).

Table 6 Semi-quantitative fine earth and clay mineralogy of the profiles

Profile and	Fine earth mineralogy					Clay mineralogy							
horizon	Q	K-Fld	Pl	Phy	Ca	K	I	Sm	Chl	V	Chl/Sm	I/Sm	Chl/V
Faidella													
Bw	89.0	0.4	-	10.5	-	25.4	5.2	-	1.6	-	-	41.0	26.7
Bwb	82.9	2.4	-	14.7	-	12.5	1.0	-	-	-	-	74.9	11.5
Sandstone	46	0.4	-	3.5	49.5	2.0	5.3	-	-	-	-	92.8	-
Comiols													
Bw	88.1	0.3	-	11.6	-	78.2	1.3	-	-	5.1	-	15.4	-
C	91.6	0.6	-	7.9	-	82.9	3.0	-	-	-	-	14.1	-
Sandstone	17.5	0.2	-	1.5	80.9	90.0	9.8	-	-	-	-	-	-
Nerets 1													
A	60.0	21.0	-	19.0	-	50.0	8.3	8.3	-	-	20.0	16.7	-
AB	67.8	3.0	2.0	27.2	-	46.7	13.3	6.7	6.5	-	19.0	6.4	-
Bt1	85.2	2.1	-	13.1	-	42.9	14.3	4.8	9.5	-	20.0	4.8	-
Bt2	37.8	15.2	5.2	41.8	-	42.1	26.3	5.3	-	-	18.0	5.3	-
Bt3	27.0	1.4	0.9	70.7	-	40.0	24.0	4.0	-	-	20.0	12.0	-
Bt4	42.3	2.6	1.8	53.3	-	88.9	4.4	0.7	-	-	19.0	2.2	-
Nerets 2													
Bt	44.8	5.2	1.4	48.6	-	33.3	25.9	3.7	-	-	20.0	11.1	-
2Btk1	57.6	2.0	0.9	39.6	-	28.6	21.4	3.6	-	-	20.0	28.6	-
2Bk2	57.8	1.1	11.4	29.7	-	50.0	50.0	-	-	-	18.0	-	-
3Bk3	50.6	15.3	22.9	11.2	-	33.3	41.7	4.2	-	-	20.0	4.2	-

Q: Quartz, K-Fld: K-Feldspar, Pl: Plagioclases, Phy: Phyllosilicates, Ca: Calcite; K: Kaolinite, I: Illite, Sm: Smectite, V: Vermiculite.

alluvial fan evolution in Nerets. Additionally, it shows that the weathering degree does not depend on the age of the geomorphic unit, which would correspond in increasing age to Faidella/Comiols/Nerets 3 and 4/surface of Nerets 2/Nerets 1.

The elemental composition of Faidella, Comiols, and Nerets 1 and 2 (Table 5) shows a downward leaching of Ca, Mg, K in all profiles, and a relative enrichment of Al and Fe in the top horizons of Nerets 2 and Comiols, while they increase in depth in Nerets 1. Faidella has an anomalous behaviour in depth, due to the buried soil. The chemical weathering and alteration indices (Nesbitt and Young, 1982; Harnois, 1988), calculated with the element content, distinguishes the original sandstones (lowest indices) from the Bk (medium indices) and from the A and Bt horizons (highest indices) of the profiles.

3.4. SOIL MINERALOGY

Table 6 presents the profile mineralogy, both of the fine earth and of the clay fraction. The fine earth is mainly composed of quartz, with varying amounts of K-feldspars and plagioclases, which were inherited from the parent material. The absence of plagioclases in the sandstones must be attributed to the resolution of the method, which could not detect the plagioclases (Table 6), even though these were identified in the thin sections (Figure 2). Most of the phyllosilicates (reaching over 70 % in the Bt3 horizon of Nerets 1) are therefore pedogenetic. They consist of kaolinite (from 30 to 80 %) and illite (1 to 50 %), with considerable amounts of mixed layers of chlorite/smectite (around 20 % in Nerets1 and 2) or illite/smectite (2 to 75%). Minor components are chlorites, smectites, and mixed layers of chlorite/vermiculite, although the latter is only present in Faidella (11 to 27 %). These results are similar to those of Bech et al. (1985), who reported a predominance of kaolinite in similar profiles of the area.

The mineralogy of the two Areny sandstone samples is very different: the one at Comiols is more calcareous (81 % calcite), and the clay (1.1 %) is composed mainly of kaolinite with a little illite. The one at Faidella is less calcareous (50 % calcite) and the clay (3.5 %) is composed of mixed layers of illite/smectite. These compositions reflect that some pedogenesis took place during an early diagenesis that was not spatially homogeneous (Díaz-Molina et al., 2007).

3.5. SOIL MICROMORPHOLOGY

The common feature in all horizons is the coarse fraction, made up of coarse to very coarse sand and gravels of rounded quartz, equant and fresh that correspond to the skeleton of the sandstone, once decarbonated. The distinctive micromorphological characteristics are displayed in Table 7.

Contrary to the clearly microlaminated clay coatings of the Nerets1 and 2 profiles, the Bw of the Comiols profile does not show clear illuviated clay coatings. Very rarely, fine moderately anisotropic, dusty clay coatings appear around the quartz sands (Figure 4a). Instead, a chitonic c/f related

Table 7 Main micromorphological characteristics of selected horizons

	Microstructure and porosity	c/f related distribution	Micromass and b-fabric	Pedofeatures
Comiols				
Bw	Pellicular grain, compound packing pores.	Chitonic.	Dark reddish clay, mottled, stipple-speckled to undifferenciated b-fabric.	Few fine, moderately anisotropic, dusty clay coatings around the quartz sand grains.
Nerets 1				
Bt	Pellicular grain / vughy. Compound packing pores and vughs.	Chitonic.	Reddish clay, mottled, undifferenciated b-fabric.	Frequent microlaminated clay coatings on pore walls.
Bt2 47-67cm	Pellicular grain / vughy. Compound packing pores and vughs.	Chitonic.	Reddish clay, mottled, undifferenciated b-fabric.	Very few microlaminated clay coatings on pore walls.
Bt2 80-93	Vughy. Vughs and vesicles.	Closed porphyric.	Reddish clay, mottled, mosaic speckled b-fabric.	Microlaminated clay coatings and infillins around coarse fragments, fragmented and incorporated to the groundmass.
Bt4	Vughy. Vughs and vesicles.	Closed porphyric.	Reddish clay, mottled, undifferenciated b-fabric.	Microlaminated clay coatings and infillins around coarse fragments, fragmented and incorporated to the groundmass.
Nerets 2				
Bt	Single grain pellicular/ vughy. Compound packing voids and vughs.	Chitonic to close porphyric.	Reddish clay, mottled, mosaic speckled and granostriated b-fabric.	Microlaminated clay coatings and infillings, with different fragmentation and deformation degrees, frequent.
Bt/2Btk1	Single grain pellicular/ vughy. Compound packing voids and vughs.	Chitonic to close porphyric.	Reddish clay, mottled, mosaic speckled and granostriated b-fabric.	(1) Microlaminated clay coatings and infillings with different fragmentation and deformation degrees, frequent. (2) Loose discontinuous infillings of micrite aggregates and microsparite (rods) in pores, superposed to (1). (3) Agregate nodules and incomplete dense infillings of calcite, pseudomorphs of plant components, irregular distribution, superposed to (1), breaking them and mixing them with calcite. (4) Nodules of Fe oxi-hydroxides, aggregate, few, associated to (3).
2Bk2	Vughy, vughs.	Close porphyric.	Grey, fine silt, clay and micrite, cristallitic micritic b-fabric.	(1) Strongly impregnated micrite hypocoatings on vugh walls, abundant. (2) Dense incomplete infillings of micrite and acicular calcite on vughs, interlaced. (3) Micrite nodule, gravel size, with internal interlaced fabric. (4) Nodules of Fe oxi-hydroxides, aggregate. (5) Coatings of silt and clay around coarse fragments, mostly on sandstone fragments, isotropic.
2Bk2 (150 cm)	Intergrain microaggregate. Vughs, compound packing pores.	Enaulic.	Grey, fine silt, clay and micrite, crystallitic micritic b-fabric.	(1) Strongly impregnated micrite hypocoatings on vugh walls, abundant. (2) Dense incomplete infillings of micrite and needle calcite in vughs, very frequent, following interlaced patterns. (3) Aggregate nodules of Fe oxy-hydroxides.
3Bk3	Id.	Id.	Id.	Id.

distribution, with a stipple-speckled to undifferentiated b-fabric is observed (Figure 4b). This is why, despite the description of some coatings in the field, we designate this horizon as Bw and consider it a cambic horizon. However, the weak anisotropy of the micromass may be due to the high Fe-dithionite (Table 4) contained in cryptocrystalline Fe-oxides, which can mask any orientation of the clay particles; therefore, clay illuviation should not be discarded.

The upper horizons of Nerets 1 (down to Bt2) have a chitonic c/f related distribution, with a reddish mottled clay as the micromass, isotropic under crossed polarizers, that covers the quartz grains. In these horizons, varying amounts of microlaminated clay coat the pore walls (Figure 4c). Below these horizons, clay illuviation, more frequent microlaminated clay coatings, and infillings around coarse fragments can be observed. They are fragmented and incorporated into the groundmass. The c/f related distribution becomes close porphyric in depth (Figure 4d).

The upper horizons of Nerets 2 are very similar to the bottom horizons of Nerets 1 (see Table 7): the micromass has a mosaic speckled and granostriated b-fabric and the clay coatings and infillings are fragmented and

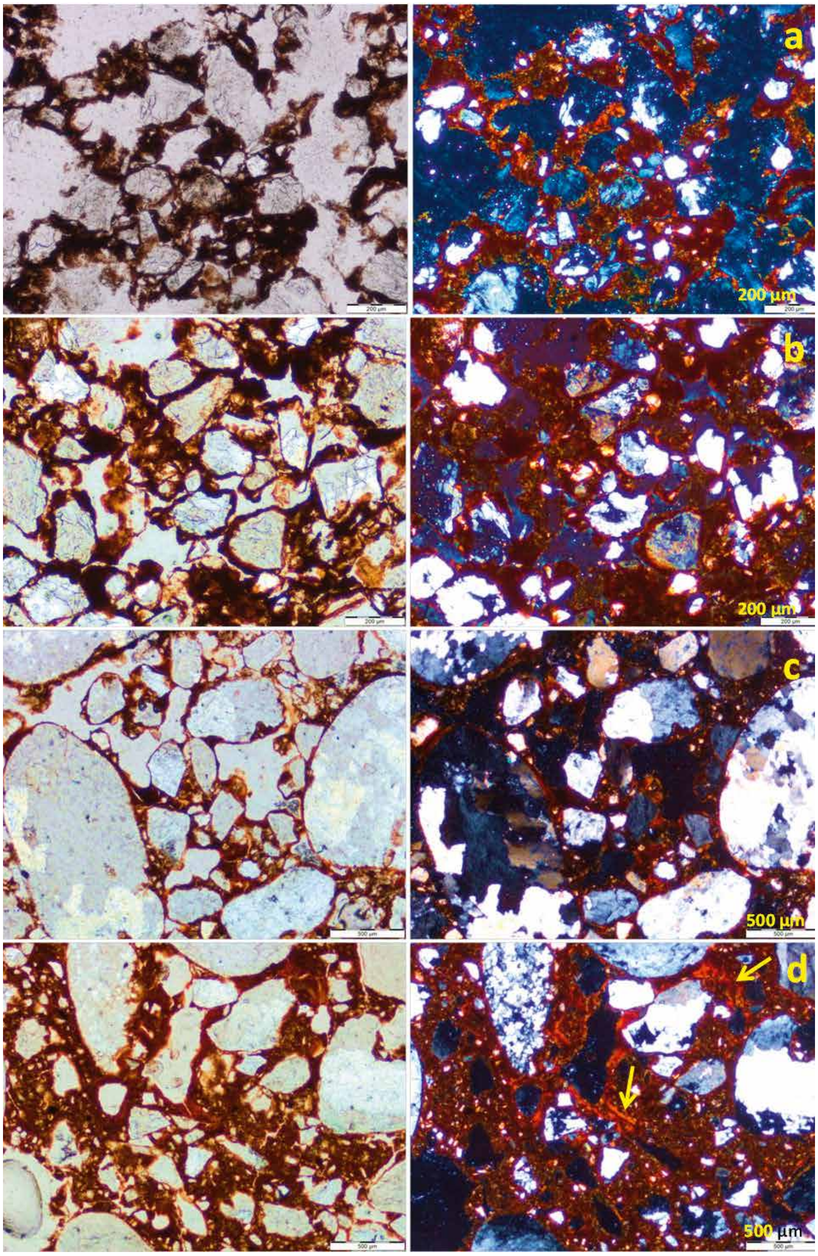

Figure 4.
a. moderately microlaminated clay coatings in Bt horizon of Comiols
b. chitonic c/f related distribution and almost undifferentiated b-fabric, probably due to an abundance in Fe oxi-hydroxides in the Bt horizon of Comiols
c. chitonic to gefuric c/f related distribution and fine microlaminated (anisotropic) clay coatings in Bt1 horizon of Nerets 1
d. progressive clogging of packing pores by micromass in Bt2 horizon of Nerets 1, resulting in a close porphyric c/f related distribution, note the clay coatings (arrows)

deformed at various degrees (Figure 5a). Below the non-carbonated part, calcitic pedofeatures are present. They are superposed to the clay coatings, breaking them and mixing them with calcite (Figure 5b). The coarse fraction of the 2Btk1 horizon contains some rounded gravels made of fragments of the original calcareous sandstone and sparite, besides the quartz grains (Figure 5c). The micromass has a micritic cristallitic b-fabric. The calcitic pedofeatures are represented by hypocoatings and needle fiber calcite (Figure 5d).

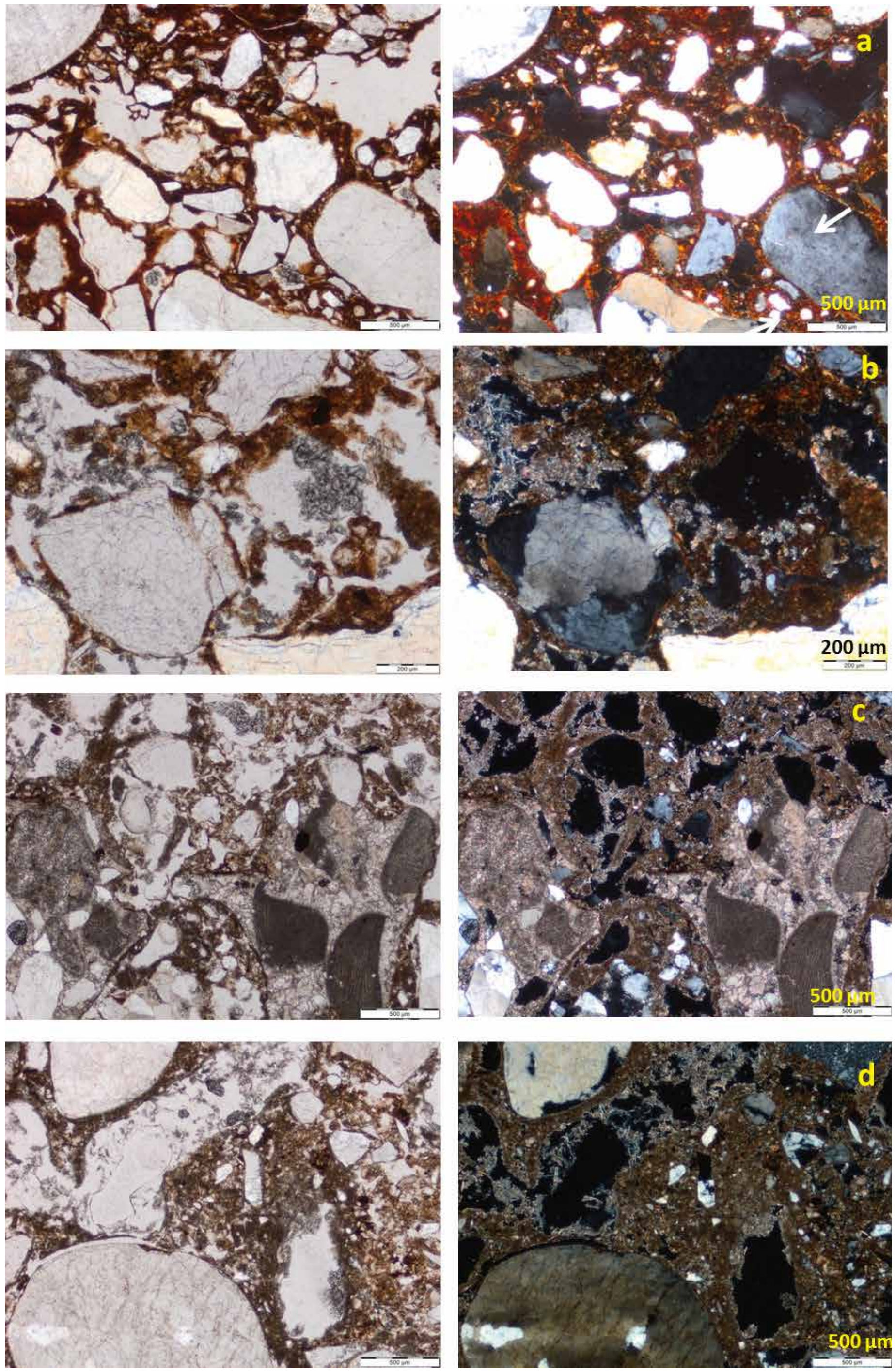

Figure 5.
a. micromass with a chitonic to close porphyric c/f related distribution and a mosaic speckled b-fabric, due to deformation and fragmentation of previous clay coatings in Bt horizon of Nerets 2
b. loose discontinuous infillings of needle calcite (upper left) and micrite coatings (lower center) in Btk2 horizon of Nerets 2
c. fragments of the original Areny sandstone in Nerets 2
d. loose discontinuous infilling of needle calcite in a channel (upper left) and micrite coating and impregnative hypocoating in a pore (lower right) in 2Bk horizon of Nerets 2, (100-110 cm)

3.6. SOIL CLASSIFICATION

Table 8 shows the classification of the six profiles according to the two international soil classification systems. According to Soil Taxonomy (SSS, 2014), Faidella and Comiols are Entisols and Inceptisols respectively, while all the profiles at the Nerets site are Alfisols (Xeralfs). This classification allows the distinction between the older Nerets 1 and 2 (Palexeralfs) and Nerets 3 and 4 (Haploxeralfs). According to WRB (IUSS Working Group WRB, 2015), Faidella and Comiols are Arenosols and Cambisols, Nerets 1 is a Lixisol and the rest are Luvisols, reflecting the result of the different durations of the soil-forming processes.

4. Discussion

An advanced weathering stage can be observed in some of the studied soils, as evidenced by the red colour (Nerets 1 in particular), the decarbonation, and by the predominance of kaolinite in the clay fraction. While the red colour might be attributed to present-day processes under a Mediterranean climate, decarbonation and kaolinite are apparently not in agreement with the climate of the area. Indeed, carbonate mobilisation and accumulation is one of the main soil-forming processes in the rest of the parent materials under the same climate. Kaolinite is the typical 1:1 clay under highly weathering environments (high temperature and high water availability throughout the year). Nevertheless, the Areny sandstone presents a higher susceptibility of being decarbonated than the neighbouring marls because of its sandy nature and partial brecciation during diagenesis (higher permeability) and because calcite is mainly present as a cement of the quartz sand.

Nevertheless, only two of the profiles (Faidella and Nerets 1) are partly decalcified. In the first case, it is due to its position at a higher altitude and consequently receiving more precipitation (Ustic regime) and lower evapotranspiration. In the second case, it is due to a limited lateral calcium-rich flow component, which in the rest of the profiles prevents decalcification and maintains the base saturation near to 100 %. In spite of that, the vertical flow has played a clear role in the decarbonation of the soils, shown by the lower depth of decarbonated horizons in the soils of the lower fan.

Regarding clay illuviation, it should be seen as the result of clay dispersion in decarbonated material, since in nearby areas in the Pyrenees, on carbonate-free parent materials, clay illuviation is a present-day process (Poch et al., 2013). It is interesting to see that neither the development degree of the clay-illuviated Bt horizons, nor the redness rating, nor the Fe-index are related to the age of the geomorphic unit, where they develop, or their altitude. This supports the thesis of a pre-weathering of the materials that were redistributed on different levels of alluvial fans during the Quaternary. The meta-analysis of Sauer (2010) reports that a time span of 100 to 300 ky is necessary to develop the redness ratings we found in Nerets profiles. These values are in the range of the age of the landform where Nerets 1 and 2 profiles are found, but not of that of Nerets 3 and 4, which is much younger, and therefore it is an indication of redistribution of pedosediments down the slope. Additionally, the Fe_d/Fe_t and $(Fe_d\text{-}Fe_{ox})/Fe_t$ indices, which can be used as age indicators in Mediterranean environments, correspond to profile developments older than 800 ky (Calabria, Scarciglia et al., 2015) or than 600 ky (Southern Spain, Martín-García et al., 2016) on surfaces of the Conca de Tremp that are actually about 350 ky (Nerets higher alluvial fan) and 50 ka (Nerets lower alluvial fan) or on slope colluvium (Faidella and Comiols profiles).

Table 8 Classification of the studied profiles according to the Soil Taxonomy (SSS,2014) and World Reference Base (IUSS Working Group WRB. 2015)

Profile	Soil Taxonomy	World Reference Base
Faidella	Typic Usthorthent	Eutric Brunic Arenosol (Colluvic, Nechic)
Comiols	Typic Haplustept	Eutric Chromic Cambisol (Loamic, Ochric)
Nerets 1	Arenic Palexeralf	Chromic Lixisol (Arenic, Cutanic, Hypereutric, Ochric)
Nerets 2	Calcic Palexeralf	Calcic Chromic Nudiargic Luvisol (Cutanic, Loamic)
Nerets 3	Calcic Haploxeralf	Calcic Chromic Luvisol (Cutanic, Loamic, Ochric)
Nerets 4	Calcic Haploxeralf	Calcic Chromic Luvisol (Cutanic, Loamic, Ochric)

5. Conclusions

The fast pedogenesis rates of the Areny sandstones, which has been taking place since its diagenesis in the Upper Cretaceous, is responsible for the lack of a correlation of the different age proxies used in Mediterranean environments (redness indices and iron ratios) with geomorphic position (geomorphic unit ages). The formation of kaolinite, karstification and partial decarbonation are considered as inherited processes, which have been acting since the pre-Quaternary period, while reddening and clay illuviation together with calcium carbonate redistribution may be more recent. The present-day soils are therefore developed on pre-weathered pedosediments that underwent some of the typical Mediterranean weathering under very different environments. This advanced pedogenesis is confronted, in the same basin, with a different pedogenetic path, i.e. calcium carbonate mobilisation and the formation of calcic and petrocalcic horizons on surfaces of similar ages developed on different materials.

Our findings allow us to conclude that the degree of development of the studied soils is controlled by the nature of the parent material, which masks, in our case, the effect of the rest of the soil-forming factors.

References

Bech, J., Garrigó, J., and Tor, F., 1985. Estudi de sòls sobre sediments maestrichtians a la conca de Tremp. *Arxius de l'ESAB,* 7, 7-22.

Bech, J., Rustullet, J., Garrigó, J., Tobias, F. J., and Martínez, R., 1997. The iron content of some red Mediterranean soils from northeast Spain and its pedogenic significance. *Catena*, 28 (3), 211-229.

Benyarku C.A. and Stoops G., 2005. *Guidelines for preparation of rock and soil thin sections and polished sections*. Quaderns DMACS, 33. Universitat de Lleida, Lleida.

CBDSA., 1983. *SINEDARES, Manual para la descripción codificada de suelos en el campo*. Ministerio de Agricultura, Pesca y Alimentación de España, Madrid.

Darwish, T.M., and Zurayk, R.A., 1997. Distribution and nature of Red Mediterranean soils in Lebanon along an altitudinal sequence. *Catena*, 28 (3), 191-202.

Díaz-Molina, M., Kälin, O., Benito, M.I., Lopez-Martinez, N., and Vicens, E., 2007. Depositional setting and early diagenesis of the dinosaur eggshell-bearing Areny Fm at Basturs, Late Campanian, South-Central Pyrenees. *Sedimentary geology*, 199 (3), 205-221.

Fedoroff, N., 1997. Clay illuviation in Red Mediterranean soils. *Catena*, 28 (3), 171-189.

Fedoroff, N. and Courty, M.A., 2013. Revisiting the genesis of red Mediterranean soils. *Turkish Journal of Earth Sciences*, 22 (3), 359-375.

Harnois, L., 1988. The CIW index- a new chemical index of weathering. *Sedimentary Geology,* 55, 319-322.

Herrero, J., Porta, J., and Fedoroff, N., 1992. Hypergypsic soil micromorphology and landscape relationships in Northeastern Spain. *Soil Science Society of America Journal*, 56 (4), 1188-1194.

Institut Cartogràfic i Geològic de Catalunya (ICGC), 2004. *Mapa Geològic de Catalunya 1:25.000. Full Vilamitjana 290-1-1*. Institut Cartogràfic i Geològic de Catalunya. Departament de Territori i Sostenibilitat, Generalitat de Catalunya, Barcelona.

Institut Cartogràfic i Geològic de Catalunya (ICGC), 2007. *Mapa geològic comarcal de Catalunya 1:50.000. Full 25 Pallars Jussà*. Institut Cartogràfic i Geològic de Catalunya. Departament de Territori i Sostenibilitat, Generalitat de Catalunya, Barcelona.

IUSS Working Group WRB, 2015. *World Reference Base for Soil Resources 2014, update 2015. International soil classification system for naming soils and creating legends for soil maps*. World Soil Resources Reports No. 106, 192. FAO, Rome.

Lewis, C.J., McDonald, E.V., Sancho, C, Peña, J.L., and Rhodes, E.J., 2009. Climatic implications of correlated Upper Pleistocene glacial and fluvial deposits on the cinca and Gállego Rivers (NE Spain) based on OSL dating and soil stratigraphy. *Global and Planetary Change*, 67, 141-152.

Linares, R., Rosell, J., Roqué, C., and Gutiérrez, F., 2010. Origin and evolution of tufa mounds related to artesian karstic springs in Isona area (Pyrenees, NE Spain). *Geodinamica Acta*, 23 (1-3), 129-150.

Machette M.N., 1985. Calcic soils of the Southwestern United States. *Geol. Soc. Am. Spec. Paper*, 203, 1-21.

MAPA, 1993. *Métodos Oficiales de Análisis.* Ministerio de Agricultura, Pesca y Alimentación de España, Madrid, Spain.

Martín-García, J.M., Sánchez-Marañón, M., Calero, J., Aranda, V., Delgado, G., and Delgado, R, 2016. Iron oxides and rare earth elements in the clay fractions of a soil chronosequence in Southern Spain. *European Journal of Soil Science*, 67 (6), 749-762.

Mehra, O.P. and Jackson, M.L., 1960. Iron oxide removal from soils and clays by a dithionite-citrate system buffered with sodium bicarbonate. *Clay and Clay Minerals*. 7, 317-327.

Mey, P.H.W., Nagtegaal, P.J.C, Roberti, K.J., and Hartevelt, J.J.A., 1968. Lithostratigraphic subdivision of post-Hercynian deposits in the South-Central Pyrenees, Spain. *Leidse Geol. Meded*., 41, 221-228.

Nesbitt, H.W. and Young, G.M., 1984. Prediction of some weathering trends of plutonic and volcanic rocks based on thermodynamic and kinetic considerations. *Geochimica et Cosmochimica Acta,* 48 (7), 1523-1534.

Oms, O., Fondevilla, V., Riera, V., Marmi, J., Vicens, E., Estrada, R., Anadón, P., Vila, B., and Galobart, À., 2016. Transitional environments of the lower Maastrichtian South-Pyrenean Basin (Catalonia, Spain): The Fumanya Member tidal flat. *Cretaceous Research*, 57, 428-442.

Pellicer, X.M., Linares, R., Gutiérrez, F., Comas, X., Roqué, C., Carbonel, D., Zarroca, M., and Rodríguez, J.A.P., 2014. Morpho-stratigraphic characterization of a tufa mound complex in the Spanish Pyrenees using ground penetrating radar and trenching, implications for studies in Mars. *Earth and Planetary Science Letters*, 388, 197-210.

Poch, R.M., Simó, I. and Boixadera, J., 2013. Benchmark soils on alluvial, fluvial and fluvio-glacial formations of the Upper-Segre valley. *Spanish Journal of Soil Science,* 3 (2),78-94.

Porta, J., Aran, M., and Boixadera, J. (Eds.), 2011. *Els sòls de Catalunya. Conca Dellà* (*Pallars Jussà*). Monografies Tècniques 1. Institut Geològic de Catalunya – Institut d'Estudis Catalans - Departament de Territori i Sostenibilitat, Generalitat de Catalunya, Barcelona.

Price, J.R. and Velbel, M.A., 2003. Chemical weathering indices applied to weathering profiles developed on heterogeneous felsic metamorphic parent rocks. *Chemical Geology,* 202 (3-4), 397-416.

Rodríguez, X. P. and Rosell, J., 1993. Contribución al conocimiento del Paleolítico inferior del Noreste de la Península Ibérica: el yacimiento de Nerets (Conca de Tremp, Catalunya). *Cuaternario y Geomorfología*, 7, 15-22.

Rosell, J., Linares, R., and Llompart, C., 2001. El "garumniense" prepirenaico. *Revista de la Sociedad Geológica de España*, 14 (1-2), 47-56.

Sancho, C., Peña, J.L., Lewis, C., McDonald, E., Rhodes, E., Pueyo, E.L., and Gosse, J., 2007. Cronología del sistema de terrazas cuaternarias en la cuenca del río Cinca (Pirineos – Depresión del Ebro). In: *Contribuciones al Estudio del Periodo Cuaternario* (Eds. J. Larrio and P.G. Silva) vol. 31-32. XII Reunión Nacional de Cuaternario (AEQUA), Ávila.

Sauer, D., Wagner, S., Brückner, H., Scarciglia, F., Mastronuzzi, G., and Stahr, K., 2010. Soil development on marine terraces near Metaponto (Gulf of Taranto, southern Italy). *Quaternary international*, 222 (1), 48-63.

Scarciglia, F., Pelle, T., Pulice, I., and Robustelli, G., 2015. A comparison of Quaternary soil chronosequences from the Ionian and Tyrrhenian coasts of Calabria, southern Italy: rates of soil development and geomorphic dynamics. *Quaternary International*, 376, 146-162.

Schwertmann, U., 1964. Differenzierung der Eisenoxide der Bodens durch photochemische Extraktion mit saurer Ammoniumoxalat-lössung. *Z. Pflanzenernähr., Düng. Bodenkd.*, 105, 194-202.

Soil Survey Staff, 2014. *Keys to Soil Taxonomy, 12th ed*. USDA-Natural Resources Conservation Service, Washington, DC.

Stoops, G., 2003. *Guidelines for analysis and description of soil and regolith thin sections*. Soil Science Society of America Inc. Madison, Wisconsin.

Torrent, J., Schwertmann, U., Fechter, H. and Alferez, F., 1983. Quantitative relationship between soil color and hematite content. *Soil Sci,* 136, 354–358.

Villalba-Breva, S., Marmi, J., Gómez, B., Daviero-Gómez, V., Martín-Closas, C., and Fernández-Marrón, M.T., 2015. Plant taphonomy and palaeoenvironment from the upper Cretaceous of Isona, Tremp basin, southern Pyrenees, Catalonia, Spain. *Cretaceous Research*, 54, 34-49.

Wagner, S., Eckmeier, E., Skowronek, A. and Günster, N., 2014. Quaternary paleosols and sediments on the Balearic islands as indicators of climate changes. *Catena* 112, 112-124.

Yaalon, D.H., 1997. Soils in the Mediterranean region: what makes them different?. *Catena*, 28 (3), 157-169.

Yousefifard, M., Ayoubi, S., Poch, R. M., Jalalian, A., Khademi, H., and Khormali, F., 2015. Clay transformation and pedogenic calcite formation on a lithosequence of igneous rocks in northwestern Iran. *Catena*, 133, 186-197.

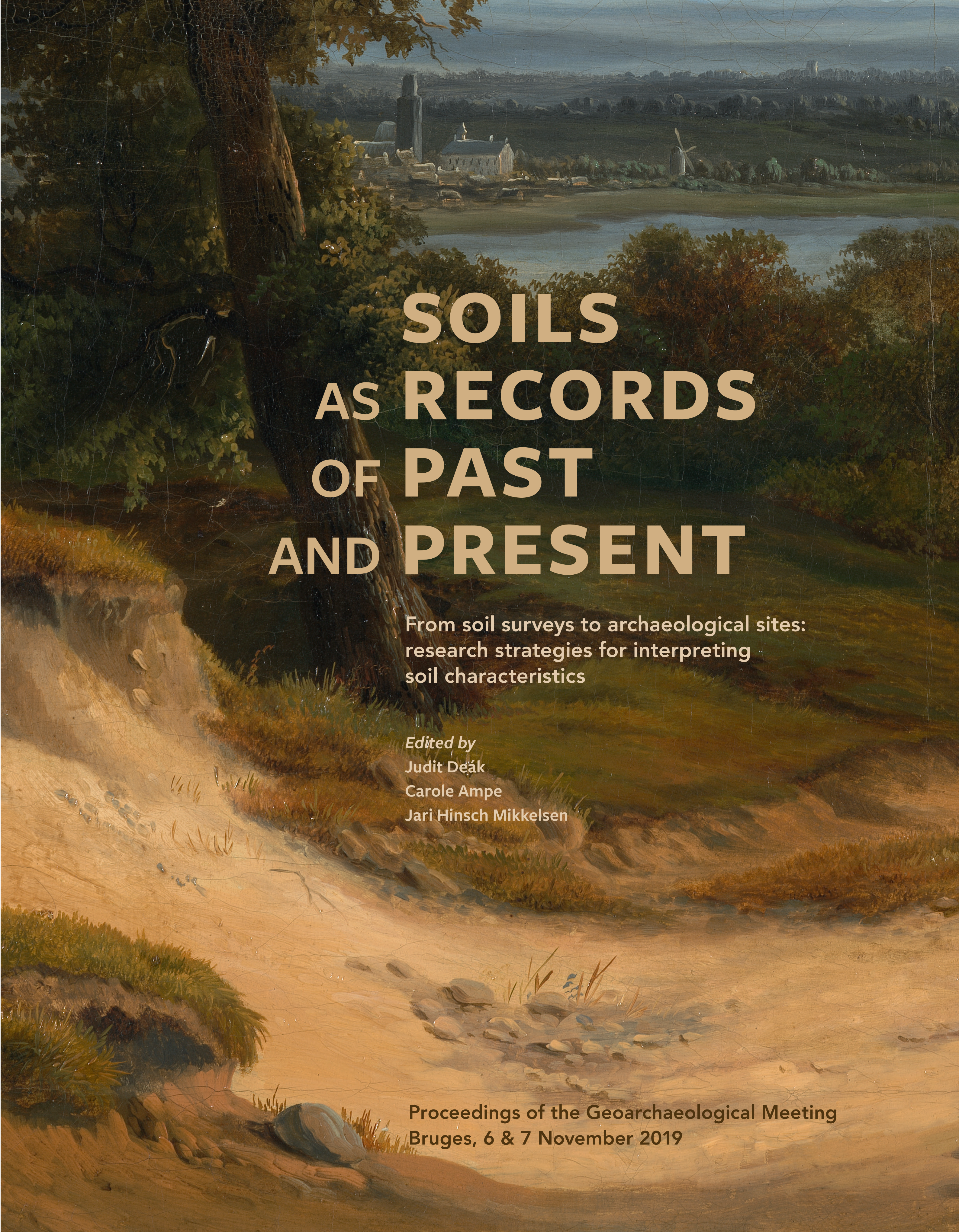

SOILS AS RECORDS OF PAST AND PRESENT

From soil surveys to archaeological sites: research strategies for interpreting soil characteristics

Edited by
Judit Deák
Carole Ampe
Jari Hinsch Mikkelsen

Proceedings of the Geoarchaeological Meeting
Bruges, 6 & 7 November 2019

This book is published on the occasion of the Geoarchaeological Meeting:

Soils as records of Past and Present.
From soil surveys to archaeological sites: research strategies for interpreting soil characteristics

on 6 & 7 November 2019 in Bruges, Belgium.

Editors
Judit Deák, Carole Ampe and Jari Hinsch Mikkelsen

Technical editor
Mariebelle Deceuninck

English language reviewer
Caroline Landsheere

Graphic design
Frederick Moyaert

Printing & binding
Die Keure, Bruges

Publisher
Raakvlak
Archaeology, Monuments and Landscapes of Bruges and Hinterland, Belgium
www.raakvlak.be

Citation recommendation
Judit Deák, Carole Ampe, and Jari Hinsch Mikkelsen (Eds.). Soils as records of past and Present. From soil surveys to archaeological sites: research strategies for interpreting soil characteristics. Proceedings of the Geoarchaeological Meeting Bruges (Belgium), 6 & 7 November, 2019. Raakvlak, Bruges.
ISBN 978 90 76297 811
Doi: http://10.5281/zenodo.3420213

TABLE OF CONTENT

3. Archaeology and soil science, unravelling the complexity

4. Past climates and environments

5. Present and future use of soil data